GLOBAL BIOGEOCHEMICAL CYCLES, VOL. 9, NO. 4, PAGES 637–651, DECEMBER 1995

Geochemistry of carbon dioxide in seawater at the Hawaii Ocean Time series station, ALOHA

Christopher L. Sabine

Atmospheric and Ocean Sciences Program, Department of Geological and Geophysical Sciences
Princeton University, Princeton, New Jersey

Fred T. Mackenzie, Christopher Winn, and David M. Karl

School of Ocean and Earth Sciences and Technology, University of Hawaii, Honolulu

Abstract. This paper examines the fundamental biological and physical processes controlling the distribution of the inorganic carbon species throughout the water column at the Hawaii Ocean Time series station, ALOHA. Profiles of alkalinity and calcium are strongly influenced by the distribution and movement of the six water masses at this location. The semiconservative behavior of these parameters can be useful in identifying water masses. The dissolution of carbonate particles, however, contributes up to 21% (49 μmol C kg^{-1}) of the dissolved inorganic carbon added to the intermediate waters between the time the waters enter the Pacific and the time they reach Station ALOHA. A sharp increase in carbonate-derived carbon observed between 800 and 2200 m is due to the dissolution of the more soluble forms of carbonate such as aragonite. The distribution of TCO_2 and pH at this site are significantly affected by biological processes as indicated by the apparent nonlinear mixing curves between water masses, the similarity of the measured ratios of C:N and C:P to the Redfield ratios in the upper 700 m of the water column, and the results of a carbon system model. The nonconservative nature of these properties demonstrates that both physical and biological factors must be considered when evaluating temporal variability. The carbon system evaluation techniques presented here are similar to those used on several previous trans-Pacific cruises allowing the results from this station to be compared to the results of other cruises in this area.

Introduction

In response to increased interest in global climate change and greenhouse warming, measurements of the marine carbon system (i.e., total CO_2, titration alkalinity, pH and pCO_2) have been included in several global research programs such as the World Ocean Circulation Experiment (WOCE) and the Joint Global Ocean Flux Study (JGOFS). These programs include both large-scale ocean surveys for looking at spatial variability and time series stations primarily designed to examine temporal variability and the mechanisms controlling this variability. Two hydrographic time series stations were established in 1988 as part of the JGOFS program. One is located in the Atlantic Ocean near Bermuda and the other is located in the Pacific Ocean near Oahu, Hawaii. The Hawaii Ocean Time series (HOT) program began in October 1988 and conducts monthly cruises to Station ALOHA, located 100 km north of Oahu, at 22°45'N, 158°00'W (Figure 1) [*Karl and Winn*, 1991]. A suite of hydrographic, biological, and chemical measurements are made throughout the water column at this site together with particle flux measurements.

There are two approaches that may be taken when attempting to evaluate the cycling of carbon in the open ocean. The approach most commonly used has been to conduct trans-ocean basin transects which can be used to make broad observations about the carbon system in that basin. Programs such as GEOSECS, NORPAX, and the Tahiti Shuttle Experiment have provided much needed information on the distribution of carbon in the Pacific Basin but have provided little information on the short-term temporal variability of the system or allowed complete evaluation of the relationships among the various carbon species. Time series programs, such as the Hawaii Ocean Time series program, provide excellent opportunities to study the temporal variability of the carbon system at a single location over several years. They provide valuable information on open ocean cycling of carbon that can be used to constrain models of the oceanic sink for CO_2. The temporal variability of the carbon system within the mixed layer and the air-sea exchange of CO_2 have been described for the first 4 years of this program [*Winn et al.*, 1994]. This paper examines the fundamental biological and physical processes controlling the distribution of the inorganic carbon species throughout the water column to be used as a basis for analyzing temporal variability below the mixed layer at the Hawaii Ocean Time series station. In particular, this work focuses on the role of carbonate production and dissolution on the carbon system. This will provide the background information necessary for future evaluations of temporal variability in the carbon system at this site.

One limitation of the single site, time series approach is the inability to evaluate the advective processes that can in-

Copyright 1995 by the American Geophysical Union.

Paper number 95GB02382.
0886-6236/95/95GB-02382$10.00

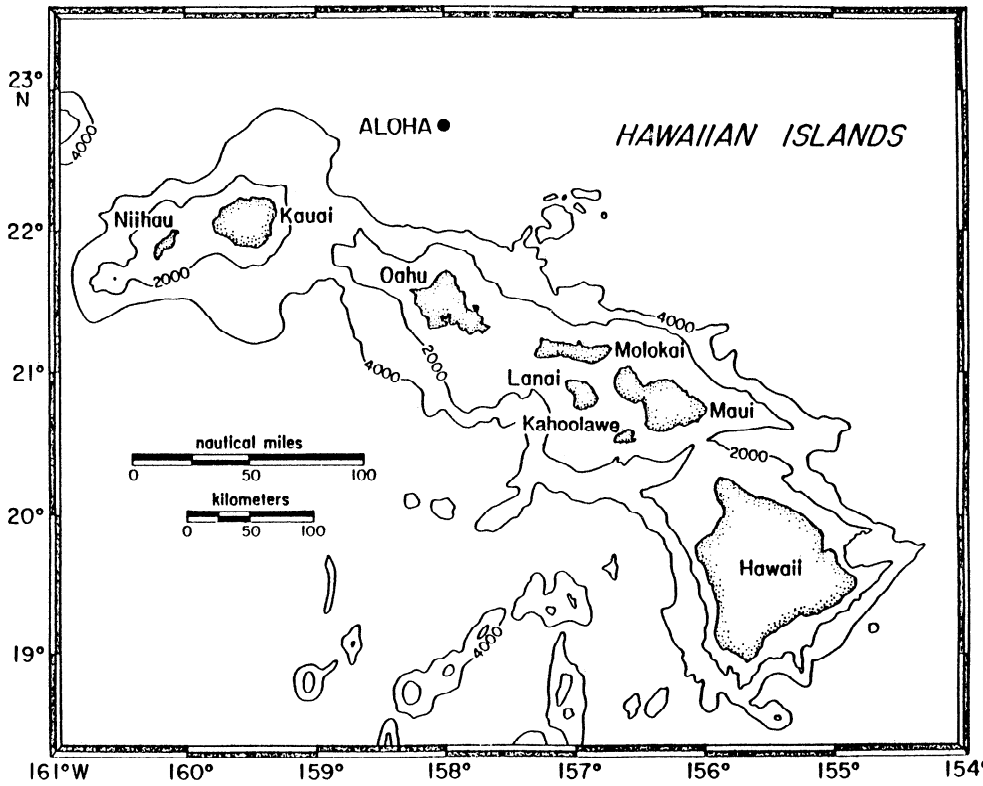


Figure 1. Map of the Hawaiian Islands showing the location of the Hawaii Ocean Time series station, ALOHA.

fluence the carbon concentrations with time. The carbon system evaluation techniques presented here are similar to those employed on several previous trans-Pacific cruises allowing the results from this station to be compared to the results of other cruises in this area. By integrating the spatial information gathered from these trans-Pacific cruises together with the temporal information from this time series station, a comprehensive evaluation of the marine carbon system is much more feasible and may be used to understand and model some of the fundamental questions of the marine carbon system.

Analytical Methodology

Water samples for dissolved oxygen, *p*H, titration alkalinity (TA), and total carbon dioxide (TCO_2) are collected approximately every month at Station ALOHA from the surface to 4600 m (bottom depth is 4750 m) using a CTD rosette system. The first 15 months of carbon data, collected from January 1989 to March 1990, are used for this analysis. Salinity values presented in this work are on the practical salinity scale.

Oxygen samples were collected in precalibrated 125-mL iodine flasks as soon as possible after the rosette arrived on deck. The entire sample was titrated using the Winkler titration procedure with visual endpoint detection [*Carpenter*, 1965]. Sample density was calculated from sample temperature measured at the time of collection. The precision of the oxygen measurements was estimated to be ±0.2 μmol kg^{-1}. Apparent oxygen utilization was calculated from the difference in the measured oxygen concentration and the equilibrium value at the potential temperature and salinity of the sample using the equations of *Weiss* [1970].

Samples for *p*H were collected in 125-mL polypropylene bottles, capped securely and placed in a water bath to bring the sample temperature to 25°C. The sample millivolt (mV) potential was measured within an hour of collection with a Corning semi-micro *p*H electrode and an Orion model EA920 ion analyzer. Sample mV readings were converted to *p*H using the measured electrode slope based on a two-point calibration in National Institute of Standards and Technology (NIST) traceable buffers and were corrected for sample temperature. The precision of the *p*H measurements was estimated to be ±0.02 *p*H units.

Alkalinity samples were titrated with a 0.1 *N* HCl solution using an automated potentiometric titration system. At least three 25-g replicates were weighed and titrated for each sample. Titration alkalinities were calculated using the Gran titration method of *Edmond* [1970] modified for automated analysis. The HCl titrant was standardized between each cruise by titrating four separate solutions prepared from primary standard grade Na_2CO_3 which was dried for 4 hours at 280°C and cooled overnight in a vacuum desiccator. The precision of the replicate alkalinity titrations was ±3 μeq kg^{-1}. Secondary standards were used to ensure the consistency of results between cruises. Analysis of these secondary standards demonstrated that the month to month precision of the alkalinities was only slightly larger than the precision of replicate titrations (±3-4 μeq kg^{-1}).

TCO_2 samples were analyzed using a modification of the coulometric procedures described by *Johnson et al.* [1985, 1987]. The coulometer used for this technique was standardized with both primary standard grade Na_2CO_3 which was dried for 4 hours at 280°C and cooled overnight in a vacuum desic-

cator and a solution of Na_2CO_3 in distilled water. The precision of this measurement was approximately ±2-3 μmol kg^{-1}.

Samples were collected for calcium determination on the October 1989 cruise (HOT-11). The calcium samples were titrated with an EGTA solution and a calcium-selective electrode using a modification of the methods developed by *Kanamori and Ikegami* [1980]. Triplicate aliquots were prepared gravimetrically and titrated for each sample. The precision of replicate titrations was ±10 μmol kg^{-1}.

Carbon system calculations were made using the carbon and carbonate dissociation constants of *Roy et al.* [1993] and *Mucci* [1983], respectively, following the procedures outlined by *Morse and Mackenzie* [1990]. These constants are based on the total seawater *p*H scale (pH_{sws}) as described by *Dickson* [1984]. Conversion of measured NIST *p*H values at 25°C to *p*H on the seawater scale (sws) at 25°C was made using the equations of *Bates and Culberson* [1977] as recommended by *UNESCO* [1983]. Values for carbonate ion concentration and *p*H at in situ temperatures and pressures were calculated using TA and *p*H measured at 25°C and 1 atm to calculate TCO_2. Since TA and TCO_2 are conservative with temperature and pressure, they were then used to calculate the carbonate ion concentrations and *p*H using the in situ temperature and pressure. The effects of pressure on the constants were determined from the ion partial molal volumes and compressibilities in seawater using the techniques outlined by *Morse and Mackenzie* [1990].

The internal consistency of the carbon system calculations was examined by comparing the species distributions calculated using different pairs of measured values (*p*H, TCO_2 and TA). Calculated values were found to agree with measured parameters within the precision of the measurements. Excellent agreement has also been observed in comparisons of alkalinity (-0.31 ±4.9 μeq kg^{-1}) and TCO_2 (0.60 ± 5.0 μmol kg^{-1}) replicates with C. D. Keeling (Scripps Institution of Oceanography, personal communication, 1992).

Water Mass Structure

The salinity structure at Station ALOHA includes a strong maximum at approximately 150 m and a minimum at around 500 m. A typical plot of potential temperature versus salinity (T-S diagram) at ALOHA readily shows linear trends inferred to be the mixing curves of five distinct water masses (Figure 2). These water masses are identified by *Chen et al.* [1987] as the North Pacific Bottom Water (NPBW), North Pacific Deep Water (NPDW), the low-salinity North Pacific Intermediate Water (NPIW), and the North Pacific Subtropical Waters which, at the latitude of Station ALOHA, can be subdivided into the Subtropical Salinity Maximum Water (STSMW) and the Subtropical Surface Water (STSW).

The shallow, high-salinity water observed at approximately 150 m (STSMW) forms in an area of excess evaporation near the subtropical front at 25° to 30°N then flows south along isopycnal surfaces. The mechanisms for the formation of this water mass and a description of its movement are thoroughly discussed by *Tsuchiya* [1968]. At Station ALOHA, the salinity values at the maximum are variable with time, ranging from 34.95 to 35.35 over this study period.

Below the salinity maximum is a prominent minimum at approximately 500 m. This salinity minimum water, designated as the North Pacific Intermediate Water (NPIW), has been extensively studied by *Reid* [1965]. Reid proposed that this water mass originates in the northwest Pacific, north of 45°N and that it is associated with the 26.8 σ_θ surface. This density surface is located at approximately 500 m at Station ALOHA. The curvature in the mixing line in the region of the salinity minimum indicates the presence of another water mass. If portions of the T-S diagram are fit with idealized straight-line mixing relationships (Figure 2), it can be shown that either there has been a complicated mixing history in the shallow portion of the salinity minimum (mixing line A on Figure 2) or an additional water mass is located between NPIW and STSMW at a potential temperature of approximately 13°C and a salinity of 34.25 (intercept of mixing line B with the STSMW mixing line on Figure 2). The first line of evidence supporting the idea of an additional water mass is that the intercept of mixing line B with the NPDW-NPIW mixing line would place the NPIW close to the 26.8 σ_θ surface as *Reid* [1965] proposed, whereas the intercept of NPDW mixing line with line A would place the NPIW on a much lower σ_θ surface. Mixing along line A would also require an asymmetrical mixing relationship between the STSMW and NPDW and a change in salinity from the original water mass of at least 0.4. The data support the conclusion that there is an additional water mass; however, it is difficult to infer definitely water mass structure from a single station.

The water mass indicated by the intersection of mixing line B with the STSMW mixing line is most likely the Shallow Salinity Minimum Water (SSMW) described by *Talley* [1985]. The SSMW forms in the eastern North Pacific as a consequence

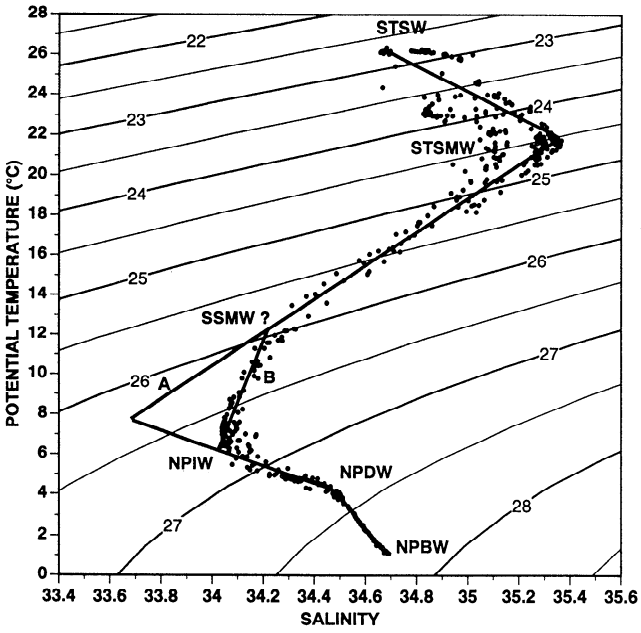


Figure 2. Plot of potential temperature versus salinity with contours of potential density. The labels A and B indicate two possible interpretations of the mixing lines. Additional labels indicate known water masses: Subtropical Surface Water (STSW); Subtropical Salinity Maximum Water (STSMW); Shallow Salinity Minimum Water (SSMW); North Pacific Intermediate Water (NPIW); North Pacific Deep Water (NPDW); North Pacific Bottom Water (NPBW).

of ventilated, wind-driven circulation. The shallow salinity minimum forms along a range of densities from 25.0 σ_θ in the easternmost outcrop to 26.2 σ_θ on the western end of the minimum. Salinity at the minimum also increases from west to east, thus resulting in a minimum where both isopycnal and isohaline surfaces cross. This structure makes simple flow interpretations impossible. However, the density range of the SSMW (around 26.2 σ_θ at Station ALOHA) would place this water mass at the proper depth to explain the intersection of line B with the STSMW mixing line.

Water Chemistry Results

Conservative Versus Nonconservative Behavior

The following discussion of the results will consider the distribution of the carbon species in terms of whether they exhibit primarily conservative or nonconservative behavior. *Sverdrup et al.* [1942] define conservative concentrations as those that are only altered by processes of diffusion and advection. Nonconservative concentrations are those altered by processes other than those of mixing and transport (e.g., biological processes). Thus a time change in concentration of the carbon species at a fixed point in the ocean is a function of advection, diffusion, and a reaction term which represents the influences of biological processes. These biological processes, which maintain the vertical TCO_2 gradient by removing carbon from the surface waters and adding carbon at depth, are hereafter referred to as the biological pump. The biological pump can be divided into two major components which *Volk and Hoffert* [1985] refer to as the carbonate and soft-tissue pumps. These terms apply to the biological production of calcium carbonate and particulate organic matter in the shallow waters and their dissolution and respiration/decay at depth, respectively. Because it is impossible to constrain all of the processes involved in maintaining the distribution of concentrations in the ocean, one must examine the actual distributions and interpret them based on knowledge gained from other sources or from the distribution itself [*Sverdrup et al.*, 1942]. It is important to remember that the observed vertical distributions do not just represent local processes but also represent the integrated signals over the historical time course of the water masses.

Titration Alkalinity

A profile of alkalinity as a function of depth at Station ALOHA exhibits a local alkalinity maximum at approximately 150 m, an alkalinity minimum at around 400 m, and then increasing alkalinity with depth (Figure 3a). The alkalinity of the deep waters, between 2000 and 4600 m, is essentially constant. The typical alkalinity profile is very similar in structure to a profile of salinity at the same site (Figure 3b). The similarity of these two profiles suggests that in general alkalinity, like salinity, behaves like a conservative tracer. One notable difference between the two profiles is the depth of the alkalinity minimum which is centered at 400 m, approximately 100 m shallower than the salinity minimum. A possible explanation for this phenomenon and its implications will be discussed later.

A profile of alkalinity normalized to a constant salinity of 35 has a very different structure from the TA profile (Figure 4). The structure of the normalized alkalinity profile resembles a typical nutrient type profile, with a surface depletion in alkalinity and regeneration at depth, suggesting that the profile is the result of nonconservative behavior (the biological pump).

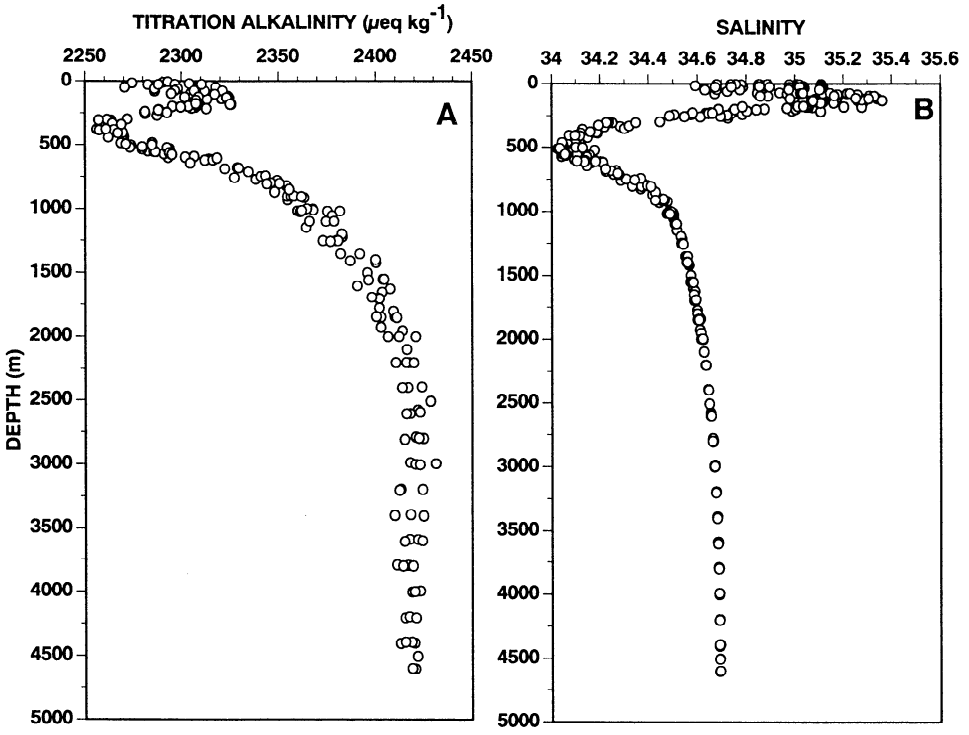


Figure 3. Profiles of (a) titration alkalinity and (b) salinity as a function of depth.

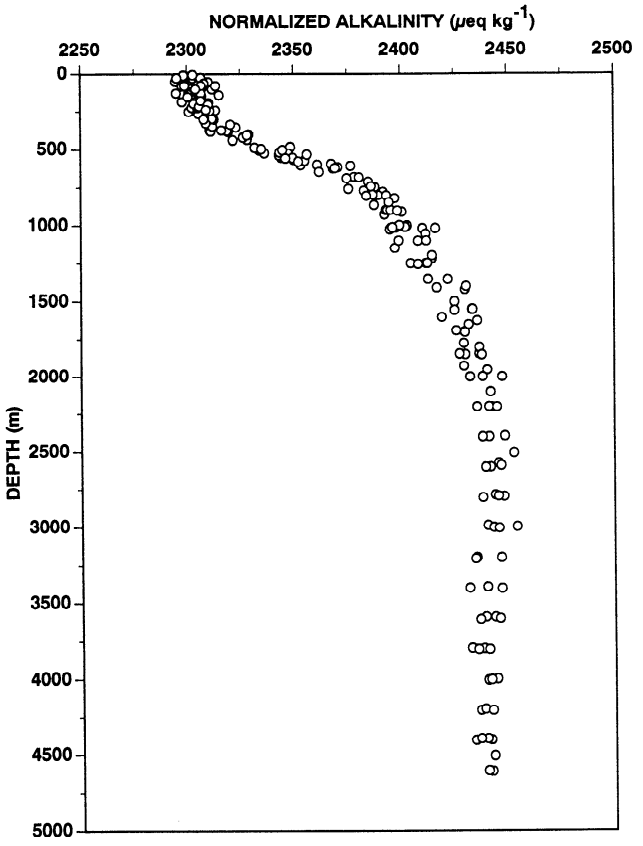


Figure 4. Profiles of titration alkalinity normalized to a constant salinity of 35 as a function of depth.

The surface waters are depleted in alkalinity because of precipitation of calcium carbonate by foraminifera, pteropods, and coccolithophoridae in the euphotic zone which generates the carbonate pump. When these organisms die, their tests sink into waters that are undersaturated with respect to the carbonate mineral phase of their skeletons. Subsequent dissolution of these tests over the historical time courses of the water masses at depth increases the alkalinity of the deeper waters, resulting in the observed normalized alkalinity profile. Titration alkalinity does not exhibit a nutrient type profile prior to normalization, suggesting that the physical processes of water mass formation and mixing occur on faster time scales than particle dissolution.

A further evaluation of the correlation between salinity and alkalinity can be made with a property-property plot of alkalinity versus salinity (A-S plot). As with the T-S diagram (Figure 2), straight mixing lines between two water mass end-members suggest conservative behavior. Although it is true that alkalinity in the deep ocean is not a true conservative tracer, because of the potential dissolution of carbonate particles in the water column, the A-S plot does exhibit linear relationships (mixing lines) between all the major water masses (Figure 5). The fact that these water masses and mixing lines can be identified suggests that the mixing processes generating these phenomena are occurring on timescales much shorter than changes in alkalinity owing to carbonate dissolution. The A-S plot, similar to a T-S diagram, shows the mixing lines between the NPBW, NPDW, NPIW, and the shallow, high-salinity waters (STSMW). The surface water mass observed with the T-S diagram (STSW) is not readily obvious from the A-S plot, because it doubles back along the mixing line for the NPIW and the STSMW. This feature makes the two mixing lines (the NPIW-STSMW and the STSMW-STSW) almost indistinguishable from each other. The two mixing lines were identified by considering only data within certain depth ranges (those data points shallower than the salinity maximum or the data points deeper than the salinity maximum) and fitting them individually with linear regressions. The slopes of the two lines were not statistically different from each other. This result indicates that although the T-S diagram shows that there are two distinct water masses shallower than the salinity minimum, these two water masses are difficult to distinguish using the A-S relationships.

The intercept of the mixing line between the surface and salinity maximum waters was not statistically different from zero. As mentioned in the previous section, the source of the salinity maximum waters is thought to be a band of excess evaporation north of Station ALOHA. Evaporation will increase the alkalinity in proportion to the salinity. Therefore, if the only factor that distinguishes the salinity maximum waters from the surface waters is evaporation, then the intercept of the mixing line between those two water masses should be zero. The constant alkalinity to salinity ratio explains why the profile of normalized alkalinity does not exhibit the alkalinity maximum observed in the TA profile. The intercept of the mixing line between the salinity maximum and salinity minimum waters (down to a salinity of 34.3), however, is 189 (± 81) μeq kg^{-1}. The positive intercept suggests that the salinity minimum waters have a higher ratio of alkalinity to salinity (specific alkalinity) than the salinity maximum waters. The higher ratio may be attributed either to a different specific alkalinity present when this water mass formed or to the addition of alkalinity from the dissolution of carbonate particles in the water mass after formation.

The question of the sixth water mass discussed in the previous section (proposed to be the shallow salinity minimum water mass described by *Talley* [1985]) can also be addressed with the A-S plot. One possibility is that the only water mass present in the area of the salinity minimum is the NPIW, which would result in mixing line A on the A-S plot (Figure 5). The intercept of the NPDW-NPIW mixing line with mixing line A indicates an initial water mass salinity of about 33.5. This result is inconsistent with the intercept of mixing line A and the NPDW-NPIW mixing line in the T-S diagram which is 0.15 higher (~33.65). The more likely situation is the presence of an additional water mass and a mixing line along B, resulting in the intercepts of the NPDW and STSMW mixing lines with line B at the same salinity values as the T-S diagram. The presence of an additional water mass also could explain the apparent difference in the depths between the salinity minimum and the alkalinity minimum. The change in salinity between the NPIW and the SSMW is reasonably large (0.2), such that the salinity minimum is obviously associated with the deeper NPIW water mass. The alkalinity of the NPIW, however, is 15 to 20 μeq kg^{-1} higher than the alkalinity of the SSMW water mass. This means that the alkalinity minimum is actually associated with the SSMW waters. This relationship creates the difference in the depth of the minimum between the salinity and alkalinity profiles.

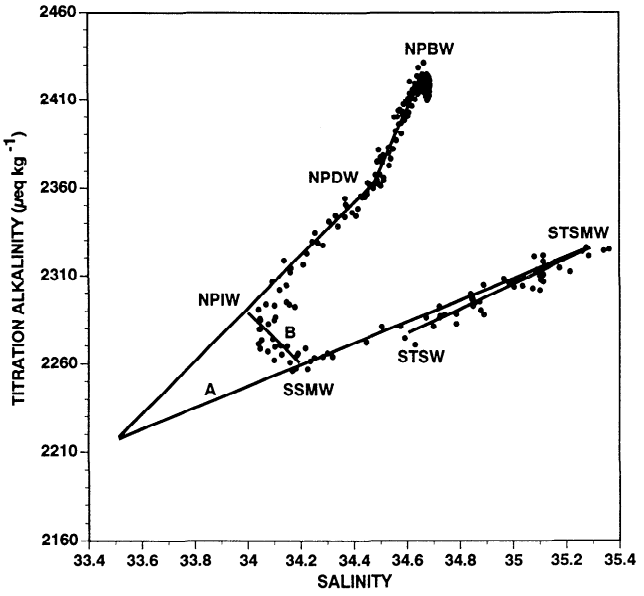


Figure 5. Plot of alkalinity versus salinity. The labels A and B indicate two possible interpretations of the mixing lines. Additional labels indicate known water masses; see Figure 2 caption.

*p*H and Apparent Oxygen Utilization

The *p*H of oceanic waters is an important indicator of biotic and physical processes occurring in the water column. The profiles of *p*H on the seawater scale at in situ temperatures and pressures have a very different structure than the alkalinity profiles (Figure 6a). Surface values for *p*H are approximately 8.05 at Station ALOHA. The *p*H values exhibit a sharp decrease with depth to approximately 700 m. Below 700 m, *p*H continuously increases with depth to the ocean bottom. Temporal variability in *p*H is very small relative to the variation in *p*H with depth. The sharp *p*H minimum at 700 m is coincident with a maximum in apparent oxygen utilization (AOU) at Station ALOHA (Figure 6b). AOU is the difference between the measured dissolved oxygen content of the water and the oxygen content that water would have if it were adiabatically raised to the surface and allowed to equilibrate with the atmosphere. This difference is a measure of oxygen consumption from the decomposition of organic matter and is negatively correlated with the dissolved oxygen concentration of the water [*Redfield*, 1942; *Jenkins*, 1982; *Chen et al.*, 1987]. Neither the AOU nor the *p*H profile exhibits a clear correlation with the water masses in the upper water column (between 0 and 1000 m). There is no evidence of the high-salinity water mass at 150 m in these profiles, and the strong AOU maximum and *p*H minimum occur between the NPIW and NPDW water masses. Although there is no practical way to separate quantitatively the relative importance of the physical processes (water mass formation and mixing) and the biological processes (soft-tissue and carbonate pumps) on the distribution with depth, a property-property plot of *p*H versus salinity demonstrates that the biological pump does affect the distribution of hydrogen ions in the water column (Figure 7). The spiral pattern of the *p*H-S plot is very different from the structure of either the T-S or A-S plots. The apparent nonlinear mixing curves between the deeper water masses suggest that *p*H is behaving nonconservatively.

The idea that *p*H is not a conservative property of ocean water is not new [*Park*, 1968; *Sugiura*, 1969]. *Park* [1968] used a

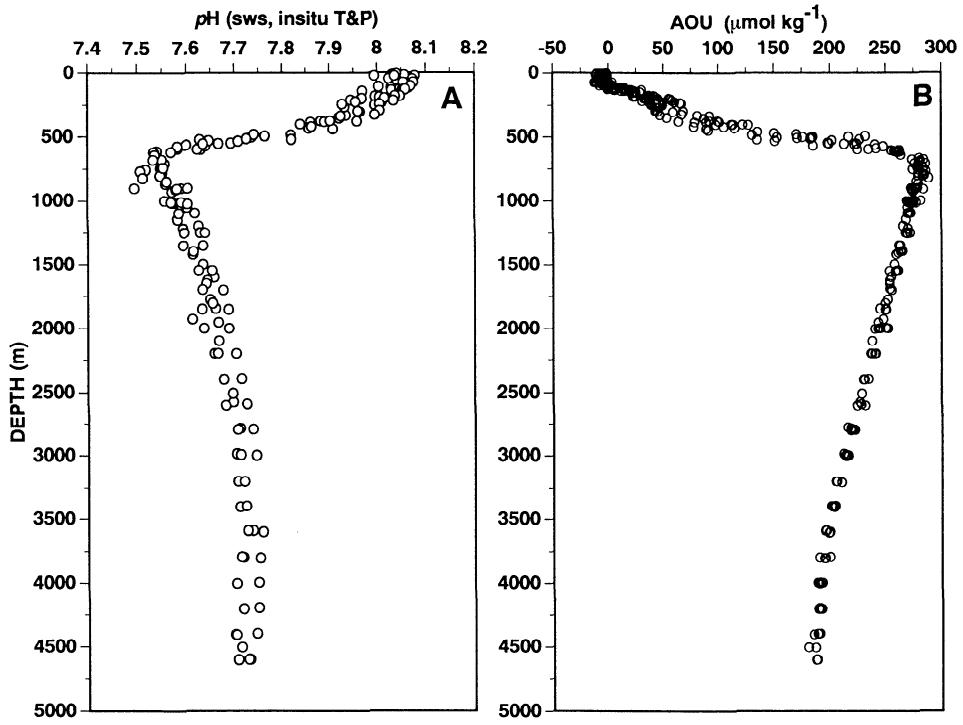


Figure 6. Profiles of (a) *p*H in the seawater scale at in situ temperatures and pressures and (b) apparent oxygen utilization as a function of depth.

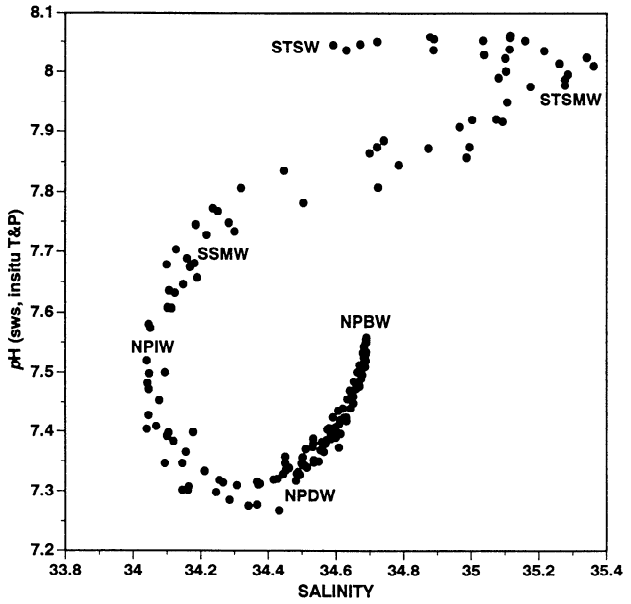


Figure 7. Plot of pH in the seawater scale at in situ temperatures and pressures versus salinity. Labels indicate the water masses discussed in the text. The horizontal placement of the labels is close to the salinity values identified on the T-S plot. The vertical placement is close to the pH values at the approximate depth of the water masses. Without specifically knowing the original pH values at the time the water masses were formed, the correct placement for the water mass labels cannot be determined. The nonlinearity of the deep water trends can be seen nonetheless.

simple one dimensional model to suggest that organic matter decomposition and carbonate dissolution were the major processes controlling the vertical hydrogen ion distribution in the northeastern Pacific. In reality, many factors may influence the pH of ocean waters including temperature, salinity, biotic activity, alkalinity, and air-sea exchange of CO_2. Biotic production and decomposition affect pH according to the following equation [e.g., *Stumm and Morgan*, 1981]

$$106CO_2 + 16NO_3^- + HPO_4^{2-} + 18H^+ + 122H_2O = (CH_2O)106(NH_3)16H_3PO_4 + 138O_2 \quad (1)$$

As organic matter is produced in the euphotic zone, hydrogen ions are consumed, increasing the pH. Although the decomposition of organic matter releases dissolved inorganic nitrogen in the form of NH_4^+ and not NO_3^-, this equation is still applicable, because the NH_4^+ generally oxidizes (nitrifies) almost completely to NO_3^- in the open ocean. When the organisms die, organic matter settles out of the euphotic zone and is oxidized generating the soft-tissue pump. Oxidation of the sinking organic matter consumes oxygen and produces protons, resulting in a decrease in the pH and an increase in AOU down to the AOU maximum/pH minimum zone.

Total Carbon Dioxide

The total carbon dioxide (TCO_2) profiles from Station ALOHA have low values in the surface waters which increase sharply with depth to about 700 m (Figure 8). Between 700 and approximately 2200 m, the TCO_2 continues to increase with depth but at a much slower rate than that in the shallow waters. Below the TCO_2 maximum at 2200 m, there is a slight decrease in TCO_2 with depth to the seafloor. As with pH, there is little correlation between the distributions of TCO_2 and the water masses in the upper water column. The water masses that result in a salinity maximum at 150 m and a salinity minimum at 500 m are not correspondingly reflected in the TCO_2 profile. A plot of TCO_2 versus salinity (Figure 9) shows the spiral pattern in the deep waters like that observed in the pH-S diagram. This apparent nonlinear behavior suggests that TCO_2 does not act conservatively in the deep waters. It could be argued, however, that the mixing curves in the upper water column (shallower than the salinity minimum waters) could be fit with linear functions. This might be interpreted as an indication that TCO_2 is acting conservatively over this depth range. Evidence suggests, however, that biology is still very important in the shallow waters. Although it is possible for physical processes to generate the observed TCO_2 gradient in the upper 700 m of the water column (Figure 8), the probability is low that the water masses would have the variable preformed TCO_2 to salinity ratios that would give a steady increase in TCO_2 despite a 0.8 increase salinity between the surface and 150 m, a 1.4 decrease in salinity between 150 and 500 m, and a 0.2 increase in salinity between 500 and 700 m. Also, the ratios of the increase in TCO_2 relative to nitrate and phosphate in the upper 700 m are 6.25 and 100, respectively. These ratios are very similar to the Redfield ratios predicted from equation (1) and within the range of values compiled by *Anderson and Sarmiento* [1994], further supporting the idea that biology plays an important role in controlling the TCO_2 distribution with depth. Unfortunately, these observations do not conclusively demonstrate the relative importance of the biological versus physical processes. To help

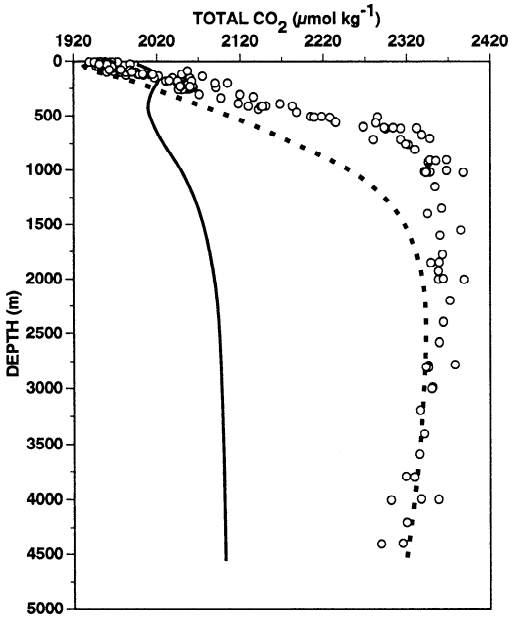


Figure 8. Profiles of TCO_2 as a function of depth. Symbols indicate direct measurements. Dashed and solid lines indicate results from a coupled carbon system-global ocean circulation model with and without biological processes, respectively.

discern the relative importance of these processes, we employed a coupled carbon system-ocean circulation model [*Sarmiento et al.*, 1995].

The carbon system model includes the physical process of gas exchange at the air-sea interface as well as the biological processes of organic matter and carbonate cycling. Air sea exchange is determined using a fixed atmospheric CO_2 concentration, the gas exchange functions of *Wanninkhof* [1992], the wind speeds of *Esbensen and Kushnir* [1981], and the carbon chemistry solution procedures of *Peng et al.* [1987]. Organic matter production and decomposition are simulated using the procedures of *Sarmiento et al.* [1988] and *Najjar et al.* [1992]. Carbonate production and dissolution are apportioned to the particulate organic carbon flux and forced to the GEOSECS horizontal mean alkalinity at each model level. The simulations use the global circulation model of *Toggweiler et al.* [1989] as modified by *Toggweiler and Samuels* [1993]. This model has 12 vertical levels and an average horizontal resolution of approximately 4°. A more thorough description of the model is given by *Sarmiento et al.* [1995].

The dashed and solid lines on Figure 8 indicate the vertical distributions of TCO_2 at Station ALOHA as simulated by the model both with and without biological processes, respectively [*Sarmiento et al.*, 1995; R. Murnane, personal communication, 1995]. The difference between these two lines indicates the biological contribution to the vertical TCO_2 gradient. These profiles are generated from 1990 mean concentrations in the 12 vertical levels of the grid box that encompasses station ALOHA. The combined model does a reasonable job of reproducing the actual measured TCO_2 profile at this site while the model without biology generates a very different TCO_2 distribution. Note that without biology the model predicts a TCO_2 profile with an increase of approximately 80 μmol kg^{-1} between the surface and 2000 m and a shallow maximum and minimum which resemble the alkalinity and salinity profiles. This structure is overwhelmed by the biology in the combined model, resulting in an increase of more than 400 μmol kg^{-1} in the upper 2000 m (see Figure 8). The relatively straight mixing lines of Figure 9, therefore, do not necessarily imply conservative behavior but could simply result from relatively large changes in salinity relative to TCO_2. The nonlinearity is much more evident in the deeper waters because the changes in salinity are smaller, and these older water masses have accumulated more TCO_2 to generate the signal.

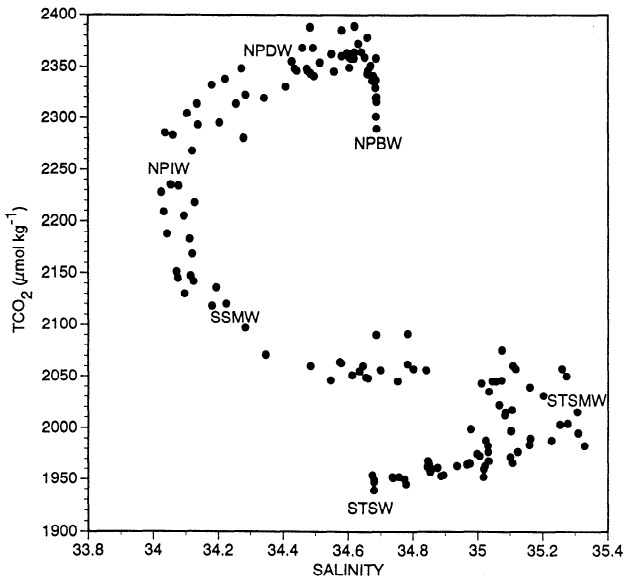


Figure 9. Plot of TCO_2 versus salinity. Labels indicate the water masses discussed in the text. The horizontal placement of the labels is close to the salinity values identified on the T-S plot. The vertical placement is close to the TCO_2 values at the approximate depth of the water masses. Without specifically knowing the original TCO_2 values at the time the water masses were formed, the correct placement for the water mass labels cannot be determined. The nonlinearity of the deep water trends can be seen nonetheless.

Dissolved Calcium and Carbonate Mineral Reactions

Eleven water samples were collected for calcium determinations from the surface to 3000 m on the October 1989 (HOT-11) cruise to Station ALOHA. Calcium concentration is an important part of the carbon system used as a variable in determining the saturation state of waters with respect to carbonate minerals and for quantifying the extent of calcium carbonate dissolution in the water column. For the purposes of saturation state calculations, it is generally considered that the calcium concentration of normal seawater is conservative with salinity [*Broecker and Peng*, 1982; *Morse and Mackenzie*, 1990]. In this case, an equation such as the following may be used to calculate the concentration of calcium in seawater:

$$mCa^{2+} = 10.28 \text{ (mmol kg}^{-1} \text{ seawater)}(S/35) \quad (2)$$

In most cases, the accuracy of this method is better than 1% and is sufficient for calculating the saturation state of the waters with respect to carbonate minerals. It has been demonstrated, however, that there is an increase in the calcium to salinity ratio with depth in the Pacific [*Horibe et al.*, 1974; *Brewer et al.*, 1975; *Tsunogai and Watanabe*, 1981]. The change in the calcium to salinity ratio is the result of the precipitation and dissolution of calcium carbonate. The excess calcium in deep waters has been used to quantify the extent of calcium carbonate dissolution [*Chen et al.*, 1987; *Chen*, 1990]. The profile of calcium at Station ALOHA is similar in shape to the alkalinity profile, with a local calcium maximum at approximately 150 m and a minimum at 400-500 m (Figure 10). As with alkalinity, the shallow maximum and minimum in the calcium profile correlate with changes in the water mass structure at the station.

A change in the calcium to salinity ratio with depth can be evaluated by comparing the profile of measured calcium to a profile of calcium calculated from salinity using equation (2) (Figure 10). There is very little difference between measured and calculated calcium concentrations for the surface waters. These concentrations begin to deviate, however, below approximately 500 m. The measured calcium concentrations increase with depth at a faster rate than the calculated calcium to a depth of 3000 m. The difference between the measured and calculated concentrations at 3000 m is 0.094 mmol kg^{-1} or about 0.9%. This difference is consistent with the findings of

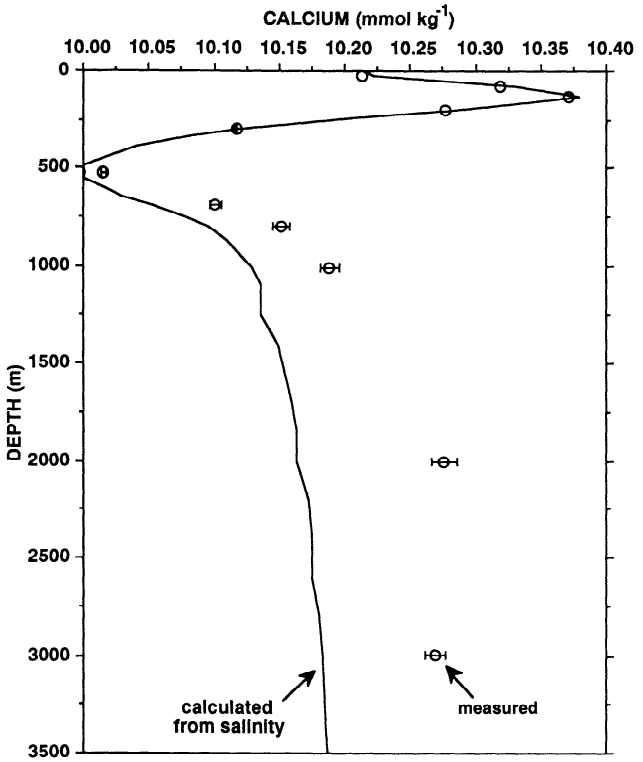


Figure 10. Profile of dissolved calcium as a function of depth. Open circles are measured values with error bars of one standard deviation based on replicate analyses. Line is calcium concentration calculated from salinity assuming a conservative relationship (from equation (2)).

other researchers, as summarized by *Morse and Mackenzie* [1990]. *Tsunogai and Watanabe* [1981], for example, found that the deep water calcium to chlorinity ratio was 0.8% higher than the warm surface water calcium to chlorinity ratio in the North Pacific.

It is generally accepted that the increase in calcium with depth is due to the dissolution of biogenically produced carbonate particles [e.g., *Kanamori and Ikegami*, 1982]. If this were true, one would expect a change in calcium concentration proportional to the change in titration alkalinity. The dissolution of $CaCO_3$ should result in a 1 mol kg^{-1} increase in Ca^{2+} for every 2 eq kg^{-1} increase in TA. However, several investigators have reported that this relationship is not observed in the open ocean [*Tsunogai et al.*, 1973; *Horibe et al.*, 1974; *Brewer et al.*, 1975]. *Kanamori and Ikegami* [1982] suggested that the difference between the expected Ca/TA ratio of 0.5 and the actual measured ratio is due to the decomposition of organic matter. Organic matter decomposition generates nitric acid which dissociates at seawater *p*H values resulting in a proton flux that, in turn, may titrate a portion of the titration alkalinity. The decrease in alkalinity would then increase the Ca/TA ratio.

The effect of organic matter decomposition can be determined from equation (1) and a consideration of how titration alkalinity is determined. The decomposition of 1 carbon equivalent mole of Redfield-type organic matter will release 16 moles of NH_4^+ into solution. In the open ocean, the NH_4^+ is oxidized to HNO_3. Because nitric acid is a strong acid, it will completely dissociate at seawater *p*H values, generating 16 moles of H^+ ions that will titrate the alkalinity of the waters. Three reactions can be written to represent the change in Ca^{2+} owing to the dissolution of carbonate (X) and the decomposition of organic matter (Y):

$$\Delta TA = 2X - 16Y \quad (3)$$

$$\Delta NO_3^- = 16Y \quad (4)$$

$$\Delta Ca^{2+} = X \quad (5)$$

Solution of the three equations yields

$$\Delta Ca^{2+} = 0.5\Delta TA + 0.5\Delta NO_3^- \quad (6)$$

The change in constituent A (ΔA) can be determined relative to a surface water sample according to

$$\Delta A = A - A_{surf}(S / S_{surf}) \quad (7)$$

This formulation assumes the possible influence of differences in the preformed values is negligible; however, this can not be truly determined without knowing the exact origin of all the water masses.

The measured ΔCa^{2+} at Station ALOHA was compared with the ΔCa^{2+} calculated solely from the change in titration alkalinity and the ΔCa^{2+} calculated from the change in titration alkalinity corrected for nitric acid. As other investigators have observed, the calcium concentrations calculated solely from the change in titration alkalinity are low relative to the measured values (Figure 11). The correction for the addition of nitric acid (equation (6)), however, corrects the Ca^{2+} values such that there is a near-perfect 1:1 relationship. It can be

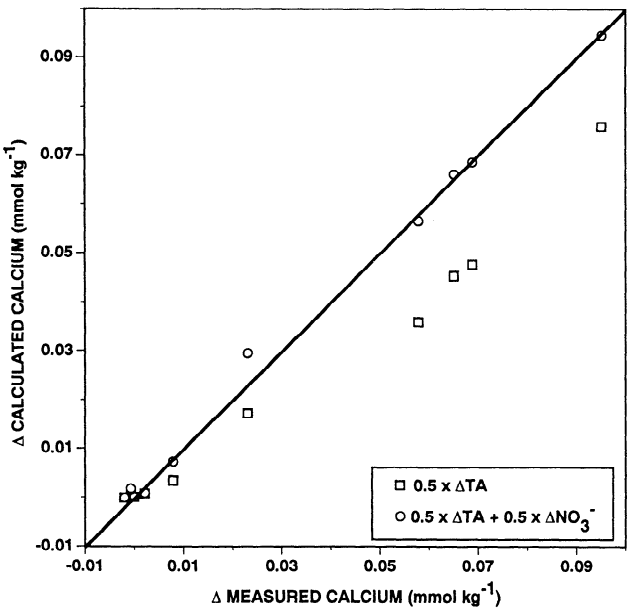


Figure 11. Plot of Δ calculated calcium verses Δ measured calcium. Delta calcium is the difference between the calcium calculated or measured at depth and the surface calcium value normalized to salinity. Calculated Δ calcium values were determined using equations described in the text.

concluded that the release of nitric acid owing to the decomposition of organic matter does significantly affect the titration alkalinity of the waters at Station ALOHA. Increases in the calcium to salinity ratio, therefore, are consistent with the increases observed in normalized alkalinity and suggest that calcium carbonate precipitation and dissolution are the fundamental processes that ultimately control the distributions of calcium and alkalinity at Station ALOHA. These data, however, do not indicate where the precipitation or dissolution has occurred. *Chen et al.* [1982b] suggested that much of the dissolved calcium in the deep Pacific, for example, was preformed and not the result of in situ dissolution. The issue of how much in situ calcium carbonate dissolution has occurred at Station ALOHA will be addressed in the next section.

Carbonate Ion Concentration and Saturation State

The distribution of carbon species can be determined from the titration alkalinity and *p*H values measured as part of this project. One of the more important species used to evaluate the relationship between carbonate particles and the carbon chemistry of the waters is the carbonate ion (CO_3^{2-}) concentration. The saturation state of the waters with respect to some carbonate phase x (Ω_x) can be determined by calculating the ratio of the measured total ion concentration product to the apparent solubility product of carbonate x (K_x). Brackets in the following equation indicate concentrations:

$$\Omega_x = [Ca^{2+}][CO_3^{2-}] / K_x \quad (8)$$

The various mineral phases of calcium carbonate each have different apparent solubility products depending on the stability of the mineral in aqueous solutions. Aragonite, for instance, is more soluble than calcite, so the ion concentration product of aragonite at equilibrium is greater than the concentration product for calcite [*Berner*, 1976; *Plummer and Busenberg*, 1982; *Sass et al.*, 1983]. The solution products of calcium carbonate are Ca^{2+} and CO_3^{2-}. Variations in carbonate ion concentrations in the ocean, however, are much greater than the variations in calcium [*Brewer et al.*, 1975; *Broecker and Peng*, 1982]. Thus the carbonate ion concentration is the primary variable determining whether or not a carbonate particle will dissolve.

Carbonate ion concentrations at in situ temperatures and pressures were calculated from *p*H and alkalinity values for each of the cruises to Station ALOHA (Figure 12). The carbonate ion concentrations are high at the surface and decrease with depth to approximately 700 m. Below 700 m the carbonate ion concentrations increase as a function of depth to the seafloor.

The solid and dashed lines on Figure 12 represent the carbonate ion concentrations at equilibrium and at 50% saturation (Ω = 0.5) with respect to calcite and aragonite, respectively. The solubility of carbonate particles increases with increasing pressure and decreasing temperature, and thus the equilibrium values increase with depth. The surface waters at Station ALOHA are well oversaturated with respect to both calcite and aragonite. Mixed layer carbonate ion concentrations are 5.5 and 3.5 times higher than the equilibrium values of calcite and aragonite, respectively. The decrease in carbonate ion concentration in the shallow oversaturated waters is primarily the

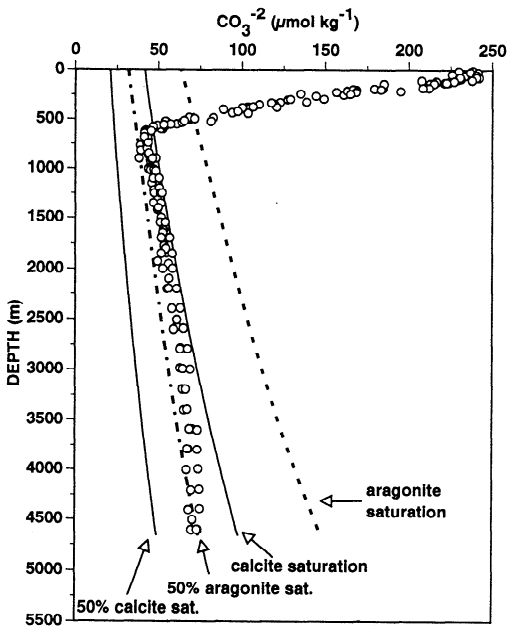


Figure 12. Carbonate ion concentration as a function of depth. Lines indicate carbonate ion concentrations at 50 and 100% saturation with respect to aragonite and calcite.

result of the decomposition of organic matter. Equation (1) shows that the decomposition of 1 mole of organic matter releases 18 moles of H^+. Some of the excess hydrogen ions in solution may then combine with carbonate ions to form bicarbonate according to

$$CO_3^{2-} + H^+ = HCO_3^- \quad (9)$$

The carbonate ion profile is similar in shape to the *p*H profile with a minimum at the same depth as the *p*H minimum and AOU maximum. This similarity suggests that the carbonate ion concentration is a nonconservative parameter.

The CO_3^{2-} concentration crosses the equilibrium value for aragonite at approximately 500 m but continues to decrease to a depth of approximately 700 m where it approaches the equilibrium value for calcite. The carbonate ion concentration remains very close to the equilibrium value for calcite to a depth of approximately 2500 m. Below 2500 m the waters become progressively more undersaturated with increasing depth. The saturation states for calcite and aragonite at Station ALOHA agree well with the results of previous studies in this area [*Chen et al.*, 1987; *Betzer et al.*, 1984; *Feely et al.*, 1984, 1988].

Previously, it was shown that the TCO_2 concentrations increase sharply with depth from the surface to about 700 m (Figure 8). In this depth range, the increase in TCO_2 relative to phosphate and nitrate was consistent with an addition of carbon from the decomposition of organic matter. Between 700 m and the TCO_2 maximum at approximately 2200 m, however, the implied C:P and C:N values are closer to 800 and 26, respectively. Although the effects of mixing cannot be discounted, the higher carbon ratios could indicate the addition of carbon over this depth range from the dissolution of calcium carbonate.

The depth range between 700 and 2200 m almost exactly corresponds with the range over which the carbonate ion concentration remains very near the equilibrium value for calcite and at 60% saturation with respect to aragonite. Although a number of factors may influence the dissolution rates of carbonate minerals, including the surface area to volume ratio and organic coatings, it has been demonstrated that the dissolution rates of calcite and aragonite increase roughly as the fourth power of the degree of undersaturation of the water [*Keir*, 1980]. Thus the dissolution rate at saturation levels close to equilibrium would be very low relative to the rate at lower saturations. *Berner* [1977] also suggested that significant undersaturation (Ω = 0.6-0.8) must be attained before dissolution of carbonate particles in the ocean will occur. Because the waters over this depth range are very near saturation with respect to calcite, it is most likely that aragonite is the primary carbonate mineral dissolving between 700 and 2200 m. The depth at which aragonitic pteropod tests are no longer found in the sediments in the central North Pacific, termed the pteropod compensation depth (PCD), is approximately 500 m [*Berger*, 1978; *Berner*, 1977], very close to the saturation depth for aragonite at Station ALOHA. Although aragonite at this depth is only slightly undersaturated, these particles may slowly dissolve at the sediment surface before they can be buried and preserved. Aragonite particles settling through the water column, however, will undoubtedly sink to greater depths before undergoing dissolution.

Betzer et al. [1984] determined from sediment trap studies in the North Pacific that the flux of pteropod aragonite at 2200 m was less than 10% of the aragonite flux at 100 m. Their estimate of the range over which aragonite dissolves exactly corresponds with the range at Station ALOHA over which carbonate dissolution appears to influence TCO_2 and the carbonate ion concentration remains very near the 60% saturation level for aragonite. Below approximately 2200 m at Station ALOHA, the carbonate ion concentration begins to deviate toward values significantly below the calcite saturation value. The constant carbonate ion concentration below 2200 to 2500 m may be a consequence of the complete dissolution of aragonite particles at shallower depths. Calcite is the only carbonate mineral found in the sediments at 2500 m [*Berger et al.*, 1976; *Berger*, 1976].

The depth at which calcite particles are no longer found in the sediments, termed the calcite compensation depth (CCD), is significantly deeper than the PCD. The CCD in the central North Pacific is approximately 4200 m [*Berger et al.*, 1976; *Berger*, 1976]. This depth is over 3500 m deeper than that of the PCD, because the carbonate ion concentration remains very close to the calcite equilibrium value over a large depth range. It is not until few aragonite particles are left to dissolve in the water column that the waters start to become undersaturated with respect to calcite. The depth range of the transition zone from high to low carbonate concentrations in the sediments is approximately 1000 m in the North Pacific [*Berger et al.*, 1976], corresponding to the depth range over which calcite particles begin to dissolve at Station ALOHA. There is no evidence in the sediments that calcite dissolution occurs in waters shallower than 3200 m. At a depth of 3200 m [*Berger et al.*, 1976], the waters at Station ALOHA are approximately 85% saturated with respect to calcite. This saturation level indicates the degree of undersaturation required for the dissolution of calcite to be kinetically favored in Pacific Ocean water.

Role Of Calcium Carbonate

To calculate the quantity of calcium carbonate that has dissolved in the water column at Station ALOHA, the change in salinity normalized titration alkalinity (ΔNTA) and TCO_2 ($\Delta NTCO_2$) must be determined. As mentioned in the previous sections, however, it is incorrect to assume that the higher deep water values are solely the result of in situ processes. The water masses present at Station ALOHA may have had different alkalinity or TCO_2 values at the time the water masses were formed. Therefore, to calculate properly the ΔNTA and $\Delta NTCO_2$ values, the preformed values (NTA° and $NTCO_2$°) must be determined. The source of deep waters to the Pacific is the Southern Ocean [*Sverdrup et al.*, 1942; *Knauss*, 1962]. It has been shown that the values of TA and TCO_2 in the Southern Ocean normalized to a salinity of 35 are linearly correlated with temperature, and that the preformed values of NTA° and $NTCO_2$° may be estimated for the deep waters of the Pacific from empirical equations that relate NTA and $NTCO_2$ to potential temperature (θ) [*Chen and Pytkowicz*, 1979]. *Chen et al.* [1987] point out, however, that the equations for NTA° and $NTCO_2$° are not appropriate for North Pacific waters shallower than the North Pacific Intermediate Water (NPIW), because the water mass distributions and origins are very complicated. No suitable preformed NTA or $NTCO_2$ equations exist for the shallow waters of the North Pacific. The equations used in this study to calculate the preformed values for the deep waters at Station ALOHA were taken from *Chen* [1990] based on the revised GEOSECS data. The equations are

$$NTA° \ (\mu eq\ kg^{-1}) = 2384 - 4.2\theta\ (\pm 9) \qquad (10)$$

$$NTCO_2° \ (\mu mol\ kg^{-1}) = 2219 - 11.0\theta\ (\pm 16) \qquad (11)$$

Although the original GEOSECS data required some corrections for an error in the titration program, the revised data are mutually consistent with data from the Atlantic, from chromatographic measurements and from calculations made with different pairs of measured parameters [*Broecker et al.*, 1982]. The accuracy and the compatibility of the revised GEOSECS data with data collected as part of this program can be inferred from the good agreement between the shipboard titration data and the manometric values determined on replicate samples by C. D. Keeling [*Brewer et al.*, 1986]. The mean difference for samples deeper than 1000 m was 4.0 ±2.9 $\mu mol\ kg^{-1}$, similar to recent comparisons of Station ALOHA data with the manometric method. A comparison of Station ALOHA normalized TA and TCO_2 values with data from the nearest GEOSECS station (212) also indicates that the average deep water values are within the estimated accuracy of the measurements.

Anthropogenic CO_2 Correction

Another important factor influencing carbonate dissolution calculations is anthropogenic CO_2. The calculated $\Delta NTCO_2$ used in the calculations may be significantly affected by the input of anthropogenic CO_2 [*Chen et al.*, 1982b]. *Chen* [1982] calculated that the quantity of anthropogenic CO_2 dis-

solved in the surface waters of the Pacific at the time of the GEOSECS expedition was as high as 43 μmol kg^{-1}. The use of preformed $NTCO_2$ values collected at that time would cause a systematic error in $\Delta NTCO_2$ calculations for waters that were formed prior to the increase in atmospheric CO_2. The anthropogenic contribution can be estimated by examining the difference between the preformed $NTCO_2$ values calculated from equation (11) and the preformed values estimated by removing the effects of the soft-tissue and carbonate pumps on the measured profile at Station ALOHA.

The contribution of organic matter decomposition and carbonate dissolution can be evaluated from the following equations based on the Redfield ratio of carbon, nitrogen, and oxygen given in equation (1) [*Redfield et al.*, 1963; *Chen and Pytkowicz*, 1979; *Chen et al.*, 1982b; *Kanamori and Ikegami*, 1982]:

$$\Delta NTCO_2 = NTCO_{2(measured)} - NTCO_2^\circ = X + 106Y \quad (12)$$

$$\Delta NTA = NTA_{(measured)} - NTA^\circ = 2X - 16Y \quad (13)$$

$$AOU = 138Y \quad (14)$$

The values of NTA° and $NTCO_2$° are the preformed values for these waters as they entered the Pacific. NTA° and $NTCO_2$° are calculated from equations (10) and (11), respectively. The terms X and Y in these equations represent the moles of calcium carbonate that have dissolved and the number of carbon equivalent moles of Redfield-type organic matter that have decomposed in the water column, respectively. Solving equations (12)-(14) for $\Delta NTCO_2$, ΔNTA, and AOU yields

$$\Delta NTCO_2 - 0.5\Delta NTA = 0.83AOU \quad (15)$$

Thus the correlation between the variables ($\Delta NTCO_2$ - 0.5ΔNTA) and AOU should have a slope of 0.83 based on the idealized Redfield ratio. One concern with the use of this plot is with the possible nonlinear effects of mixing on the AOU signal. These effects are minimized, however, by only considering the North Pacific Deep and Bottom Waters. These deep waters generally do not mix with waters warmer than 10°C; thus *Chen et al.* [1982a] determined that the potential error in AOU is less than 3 μmol kg^{-1}. *Chen and Pytkowicz* [1979] first postulated that the nonzero intercept in a plot of $\Delta NTCO_2$ -0.5ΔNTA versus AOU was due to the difference between the $NTCO_2$° value (the preformed value the waters would have if they were formed at the time of GEOSECS) and the actual preformed value which was formed in preindustrial times before the anthropogenic CO_2 increase.

Figure 13 is a plot of $\Delta NTCO_2$ - 0.5ΔNTA versus AOU for depths at Station ALOHA greater than 800 m. Values from depths shallower than 800 m have a different slope and approach a $\Delta NTCO_2$ - 0.5ΔNTA of zero at the surface as expected. A regression of the points deeper than 800 m yields a slope of 0.89 (± 0.02), a value very similar to the slope predicted from equation (15) above. The intercept of the regression has a value of -48.36 μmol kg^{-1} (± 4.2). This value represents the excess CO_2 that entered the surface ocean between preindustrial times and the time of the GEOSECS expedition. This value only gives the CO_2 at the time of the GEOSECS

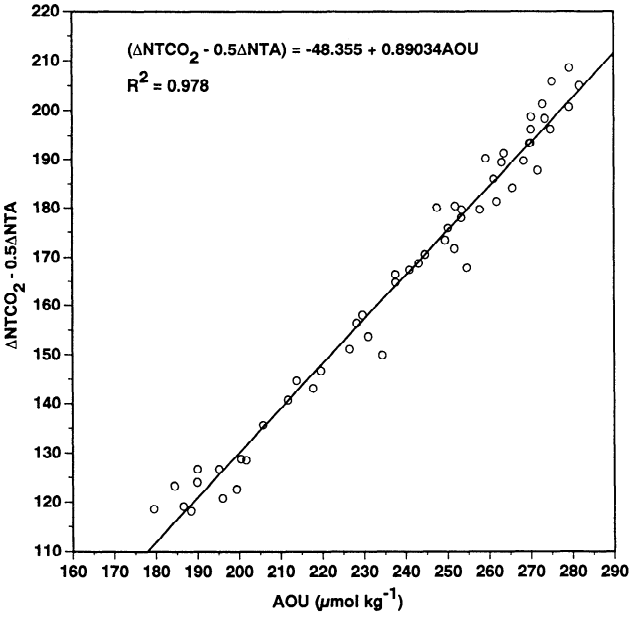


Figure 13. Plot of $\Delta NTCO_2$-0.5ΔNTA versus AOU for depths greater than 800 m. The equation and corresponding line are the best fit through the data based on a model 1 linear regression.

expedition, because the preformed equations are based on data collected at that time. The value of 48 μmol kg^{-1} is very similar to the value of 43 μmol kg^{-1} calculated by *Chen* [1982]. Despite the fact that Chen's calculations were made nearly a decade ago, the residence time of the deep Pacific is so long that the chemistry of those waters should not have significantly changed since that time. There are many uncertainties associated with these calculations which have been extensively discussed in the literature [*Brewer*, 1978; *Chen and Millero*, 1979; *Chen and Pytkowicz*, 1979; *Shiller*, 1981; *Chen*, 1982; *Chen et al.*, 1982a]. Despite the difficulties, however, they provide at least an estimate of the potential contribution of anthropogenic CO_2.

Inorganic- and Organic-Derived Carbon

Given the preformed values for NTA and $NTCO_2$ in a body of water and its present values, it is possible to determine the ratio of in situ inorganic and organic carbon decomposition. Using equations (12) and (13) above, the ratio of carbon derived from the dissolution of calcium carbonate (IC) to carbon derived from the decomposition of organic matter (OC) can be calculated from the following equation [*Chen et al.*, 1982a, 1987; *Chen*, 1990]:

$$IC/OC = X/106Y$$
$$= (0.16038\Delta NTCO_2 + \Delta NTA)/(2\Delta NTCO_2 - \Delta NTA) \quad (16)$$

As mentioned earlier, however, the $\Delta NTCO_2$ values must be corrected for the injection of anthropogenic CO_2. Failure to correct the $NTCO_2$ values for anthropogenic CO_2 could result in an error of 0.05-0.07 in the inorganic carbon to organic carbon ratio [*Chen*, 1990]. The $\Delta NTCO_2$ equation from (12) may be modified to

$$\Delta NTCO_2 = NTCO_{2(measured)} - NTCO_2^\circ + 48 \quad (17)$$

The inorganic carbon to organic carbon ratio (IC/OC) was calculated for waters deeper than 800 m from each cruise to Station ALOHA (Figure 14). The data from shallower than 800 m were not included, because the water masses present at those depths were formed in the North Pacific and not the Weddell Sea. Equations (10) and (11), therefore, are not appropriate for determining the preformed values for NTA and $NTCO_2$. The IC/OC increases from 0.13 at 800 m to approximately 0.27 at 2500 m. Below 2500 m the IC/OC remains constant to the seafloor. The constant IC/OC below 2500 m is consistent with the findings of *Chen* [1990]; however, the calculated IC/OC value of 0.27 is slightly lower than that of 0.36 calculated by Chen. An IC/OC value of 0.27 indicates that approximately 21% of the carbon in the deep Pacific is contributed from the dissolution of carbonate particles. This percentage is consistent with the findings of other researchers who have calculated the percentage of inorganic carbon in the deep Pacific owing to carbonate dissolution; for example, *Edmond* [1974] and *Ben-Yaakov* [1972] calculated values of 20.6% and 20%, respectively. These findings demonstrate that far more carbon is added to the deep ocean from the decomposition of organic matter than from the dissolution of carbonates. The increase in IC/OC with depth, however, indicates that carbonate dissolution increases as a function of depth relative to the rate of organic decomposition. This is consistent with saturation state calculations which demonstrated that the deep waters were more undersaturated with respect to carbonate than the shallow waters.

The quantity of inorganic carbon in the water column contributed by the dissolution of carbonate particles (carbonate inorganic carbon, CIC) can be calculated from equations (12) and (13) above:

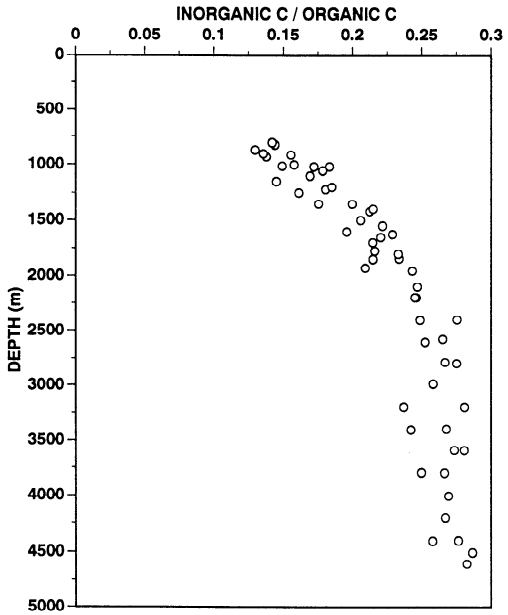


Figure 14. Plot of the ratio of carbon contributed to the waters from inorganic and organic sources below 800 m as a function of depth.

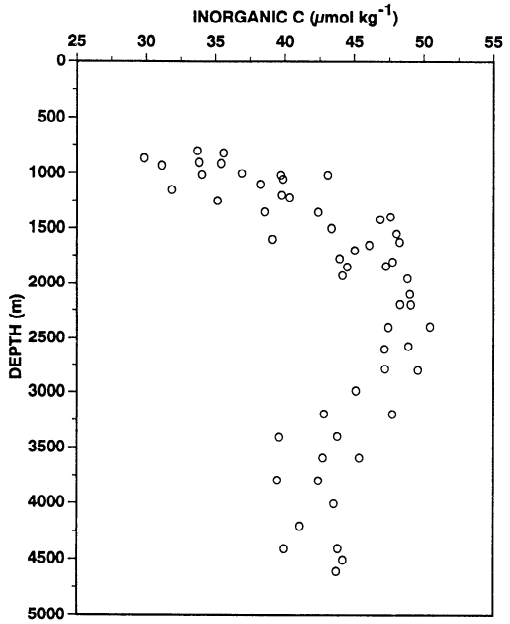


Figure 15. Plot of inorganic carbon contributed to the waters from the dissolution of calcium carbonate below 800 m as a function of depth.

$$CIC = X = 0.07424\Delta NTCO_2 + 0.4629\Delta NTA \quad (18)$$

The profile of CIC below 800 m from Station ALOHA is presented in Figure 15. The CIC at 800 m is approximately 30 μmol kg^{-1}, increasing to a maximum of approximately 49 μmol kg^{-1} at 2500 m. Between 2500 and 3500 m, the CIC decreases as a function of depth. Below 3500 m, the CIC is essentially constant to the seafloor. The increase in CIC below 800 m demonstrates that the dissolution of carbonate particles as they sink through the water column is increasing with depth. The depth of the CIC maximum is coincident with the estimated maximum depth at which aragonite particles are found in sediment trap samples, but it is shallower than the depth at which calcite dissolution is evident in the sediments. This increase in CIC, therefore, must be primarily due to the dissolution of aragonite particles. Below 2500 m, there are not as many soluble carbonate particles sinking through the water column to contribute carbon, and thus less inorganic carbon is added. The depth at which the percent calcite begins to decrease in the sediments in this area of the Pacific is approximately 3200 m [*Berger et al.*, 1976]. Therefore significant dissolution of calcite probably occurs below this depth. Thus the relatively constant CIC values observed between 3500 m and the seafloor are due to the dissolution of calcite in the bottom waters and on the seafloor.

Conclusions

The results of this study demonstrate the relative importance of the three major processes controlling the distribution of inorganic carbon at the Hawaii Ocean Time series station, ALOHA: organic matter production and decomposition, carbonate production and dissolution, and water mass distribution. The apparent nonlinear mixing curves between water

masses, the similarity of the measured ratios of C:N and C:P to the Redfield ratios in the upper 700 m of the water column, and the results of a carbon system model indicate that biological processes have a significant effect on the distribution of TCO_2 and pH values at this site. The nonconservative nature of these properties demonstrates that both physical and biological factors must be considered when evaluating temporal variability.

The profiles of alkalinity and calcium are most strongly influenced by the distribution and movement of the six water masses at this location. The shallow alkalinity and calcium maximums, for example, are features of excess evaporation near the subtropical front where this water mass is ventilated. The semiconservative behavior of these properties can be useful in identifying water masses. The differences between the depth of the alkalinity and salinity minimums at Station ALOHA help demonstrate that there are two identifiable water masses between the STSMW and the NPDW.

Although alkalinity is strongly influenced by water mass distribution and movement, a relative increase in calcium over alkalinity with depth indicates that the proton flux from the decomposition of organic matter in the water column has a measurable effect on alkalinity. The dissolution of carbonate particles also contributes to the increase in salinity normalized alkalinity with depth. Up to 21% (49 μmol C kg^{-1}) of the dissolved inorganic carbon added to the intermediate waters between the time the waters enter the Pacific and the time they reach Station ALOHA results from the dissolution of carbonate particles. The sharp increase in carbonate-derived carbon between 800 and 2200 m is due to the dissolution of the more soluble forms of carbonate such as aragonite. The waters over this depth range are at approximately 60% saturation with respect to aragonite. These particles may begin to play a more important role in the regional and global carbon cycle in the future as the oceans continue to take up anthropogenic CO_2 from the atmosphere.

Several studies have presented evidence which suggests that carbonate dissolution may increase in the Pacific as a result of rising atmospheric CO_2 [e.g., *Sabine and Mackenzie*, 1991; *Sabine*, 1992; *Feely and Chen*, 1982; *Feely et al.*, 1984; *Chen et al.*, 1987]. Aragonite compensation depths in the Pacific range between 0.5 and 1.5 km [*Berger*, 1978]. *Chen et al.* [1987] determined that fossil fuel CO_2 has penetrated to a maximum depth of 2000 m in portions of the Pacific. Thus it is likely that anthropogenic CO_2 may already be dissolving aragonite minerals suspended in the water column and in the sediments. This issue as well as a closer examination of temporal variability in the carbon system below the mixed layer will be addressed in the future. This work represents the first step toward a quantitative understanding of the open ocean carbon system in the central North Pacific Gyre.

Acknowledgments. We thank all of the HOT program personnel and cruise participants who helped to collect and analyze samples. In particular, we thank D. Hebel, who analyzed the TCO_2 samples; J. Resing for analyzing the calcium samples; and R. Murnane for providing model results for Station ALOHA. We also thank J. Morse and two anonymous reviewers for their constructive comments and suggestions for improving the manuscript. This research was funded by NSF grants EAR-8816350 (F.T.M.), EAR-8915536 (F.T.M.), OCE-8717195 (awarded to R. Lukas, E. Firing, and S. Chiswell), OCE-8800329 (D.M.K. and C.W.), the Project Development Fund of the University of Hawaii, NOAA grant NA-90-RAH-00074 (C.W., F.T.M. and D.M.K.), and DOE grant DE-FG02-93ER61540. School of Ocean and Earth Science and Technology Contribution number 3921.

References

Anderson, L. A., and J. L. Sarmiento, Redfield ratios of remineralization determined by nutrient data analysis, *Global Biogeochem. Cycles, 8*, 65-80, 1994.

Bates, R. G., and C. H. Culberson, Hydrogen ions and the thermodynamic state of marine systems, in *The Fate of Fossil Fuel CO_2 in the Oceans*, edited by N. R. Anderson and A. Malahoff, pp. 45-61, Plenum, New York, 1977.

Ben-Yaakov., S., On the CO_2-O_2 system in the northeastern Pacific, *Mar. Chem., 1*, 3-26, 1972.

Berger, W. H., Biogenous deep sea sediments: Production, preservation and interpretation, in *Chemical Oceanography*, vol. 2, edited by J. P. Riley and R. Chester, pp. 265-327, Academic, San Diego, Calif., 1976.

Berger, W. H., Deep-sea carbonate: Pteropod distribution and the aragonite compensation depth, *Deep Sea Res., 25*, 447-452, 1978.

Berger, W. H., C. G. Adelseck, and L. A. Mayer, Distribution of carbonate in surface sediments of the Pacific Ocean, *J. Geophys. Res., 81*, 2617-2627, 1976.

Berner, R. A., The solubility of calcite and aragonite at one atmosphere and 34.5 parts per thousand, *Am. J. Sci., 276*, 713-730, 1976.

Berner, R. A., Sedimentation and dissolution of Pteropods in the ocean, in *The Fate of Fossil Fuel CO_2 in the Oceans*, edited by N. R. Anderson and A. Malahoff, pp. 243-260, Plenum, New York, 1977.

Betzer, P. R., R. H. Byrne, J. G. Acker, C. S. Lewis, R. R. Jolley, and R. A. Feely, The oceanic carbonate system: A reassessment of biogenic controls, *Science, 226*, 1074-1077, 1984.

Brewer, P. G., Direct observation of the oceanic CO_2 increase, *Geophys. Res. Lett., 5*, 997-1000, 1978.

Brewer, P. G. , G. T. F. Wong, M. P. Bacon, and D. W. Spencer, An oceanic calcium problem?, *Earth Planet. Sci. Lett., 26*, 81-87, 1975.

Brewer, P. G., A. L. Bradshaw, and R. T. Williams, Measurements of total carbon dioxide and alkalinity in the North Atlantic Ocean in 1981, in *The Changing Carbon Cycle: A Global Analysis*, edited by J. R. Trabalka and D. E. Reichle, pp. 348-370, Springer-Verlag, New York, 1986.

Broecker, W. S., and T. H. Peng, *Tracers in the Sea*, 690 pp., Eldigio, Palisades, N. Y., 1982.

Broecker, W. S., D. W. Spencer and H. Craig, *GEOSECS Pacific Expedition*, vol. 3, *Hydrographic Data 1973-1974*, 137 pp., U. S. Gov. Print. Office, Washington, D. C., 1982.

Carpenter, J. H., The accuracy of the winkler method for dissolved oxygen analysis. *Limnol. and Ocean., 10*, 141-143, 1965.

Chen, C. T., Oceanic penetration of excess CO_2 in a cross section between Alaska and Hawaii, *Geophys. Res. Lett., 9*, 117-119, 1982.

Chen, C. T., Rates of calcium carbonate dissolution and organic carbon decomposition in the North Pacific Ocean, *J. Oceanogr. Soc. Jpn., 46*, 201-210, 1990.

Chen, C. T., and F. J. Millero, Gradual increase of oceanic carbon dioxide, *Nature, 277*, 205-206, 1979.

Chen, C. T., and R. M. Pytkowicz, On the total CO_2-titration alkalinity-oxygen system in the Pacific Ocean, *Nature, 281*, 362-365, 1979.

Chen, C. T., F. J. Millero, and R. M. Pytkowicz, Comment on calculating the oceanic CO_2 increase: A need for caution by A. M. Shiller, *J. Geophys. Res., 87*, 2083-2085, 1982a.

Chen, C. T., R. M. Pytkowicz, and E. J. Olson, Evaluation of the calcium problem in the South Pacific, *Geochem. J., 16*, 1-10, 1982b.

Chen, C. T., M. R. Rodmen, C. L Wei, E. J. Olson, R. A. Feely, and G. F. Gendron, Carbonate chemistry of the North Pacific Ocean, Rep. *NDP-029*, Carbon Dioxide Inf. Anal. Cent., Oak Ridge Nat. Lab., Oak Ridge, Tenn., 1987.

Dickson, A. G., pH scales and proton-transfer reactions in saline media such as seawater, *Geochim. Cosmochim. Acta, 48*, 2299-2308, 1984.

Edmond, J. M., High precision determination of titration alkalinity and total carbon dioxide content of seawater by potentiometric titration, *Deep Sea Res., 17*, 737-750, 1970.

Edmond, J. M., On the dissolution of carbonate and silicate in the deep ocean, *Deep Sea Res., 21*, 455-479, 1974.

Esbensen, S. K., and Y. Kushnir, The heat budget of the global ocean:

An atlas based on estimates from surface marine observations, *Clim. Res. Inst. Rep. 29*, Oreg. State Univ., Corvallis, 1981.

Feely, R. A., and C. T. Chen, The effect of excess CO_2 on the calculated calcite and aragonite saturation horizons in the northeast Pacific, *Geophys. Res. Lett., 9*, 1294-1297, 1982.

Feely, R. A., R. H. Byrne, P. R. Betzer, J. F. Gendron, and J. G. Acker, Factors influencing the degree of saturation of the surface and intermediate waters of the North Pacific Ocean with respect to aragonite, *J. Geophys. Res., 89*, 10631-10640, 1984.

Feely, R. A., R. H. Byrne, J. G. Acker, P. R. Betzer, C. T. Chen, J. F. Gendron, and M. F. Lamb, Winter-summer variations of calcite and aragonite saturation in the northeast Pacific, *Mar. Chem., 25*, 227-241, 1988.

Horibe, Y., K. Endo, and H. Tsubota, Calcium in the South Pacific, and its correlation with carbonate alkalinity, *Earth Planet. Sci. Lett., 23*, 136-140, 1974.

Jenkins, W. J., Oxygen utilization rates in North Atlantic subtropical gyre and primary production in oligotrophic systems, *Nature, 300*, 246-248, 1982.

Johnson, K. M., A. E. King, and J. M. Sieburth, Coulometric TCO_2 analyses for marine studies; an introduction, *Mar. Chem., 16*, 61-82, 1985.

Johnson, K. M., J. M. Seiburth, P. J. L. Williams, and L. Brandstrom, Coulometric total carbon dioxide analysis for marine studies: Maximizing the performance of an automated gas extraction system and coulometric detector, *Mar. Chem., 21*, 117-133, 1987.

Kanamori, S., and H. Ikegami, Computer processed potentiometric titration for the determination of calcium and magnesium in sea water, *J. Oceanogr. Soc. Jpn., 36*, 177-184, 1980.

Kanamori, S., and H. Ikegami, Calcium-alkalinity relationship in the North Pacific, *J. Oceanog. Soc. Jpn., 38*, 57-62, 1982.

Karl, D. M., and C. D. Winn, A sea of change: Monitoring the oceans' carbon cycle, *Environ. Sci. Technol., 25*, 1976-1981, 1991.

Keir, R. S., The dissolution kinetics of biogenic calcium carbonates in seawater, *Geochim. Cosmochim. Acta, 44*, 241-252, 1980.

Knauss, J. A., On some aspects of the deep circulation in the Pacific, *J. Geophys. Res., 67*, 3943-3954, 1962.

Morse, J. W., and F. T. Mackenzie, *Geochemistry of Sedimentary Carbonates*, 750 pp., Elsevier, New York, 1990.

Mucci, A., The solubility of calcite and aragonite in seawater at various salinities, temperatures and one atmosphere total pressure, *Am. J. Sci., 283*, 780-799, 1983.

Najjar, R. G., J. L. Sarmiento, and J. R. Toggweiler, Downward transport and fate of organic matter in the oceans: Simulations with a general circulation model, *Global Biogeochem. Cycles, 6*, 45-76, 1992.

Park, P. K., Seawater hydrogen-ion concentration: Vertical distribution, *Science, 162*, 357-358, 1968.

Peng, T. H., T. Takahashi and W. S. Broecker, Seasonal variability of carbon dioxide, nutrients and oxygen in the northern North Atlantic surface water: Observations and a model, *Tellus, 39B*, 439-458, 1987.

Plummer, L. N., and E. Busenberg, The solubilities of calcite, aragonite and vaterite in CO_2-H_2O solutions between 0 and 90°C and an evaluation of the aqueous model for the system $CaCO_3$-CO_2-H_2O, *Geochim. Cosmochim. Acta, 46*, 1011-1040, 1982.

Redfield, A. C., The processes determining the concentrations of oxygen, phosphate and other organic derivatives within the depths of the Atlantic Ocean, *Pap. Phys. Oceanogr. Meterol., 9*, 1-22, 1942.

Redfield, A. C., B. H. Ketchum, and F. A. Richards, The influence of organisms on the composition of sea water, in *The Sea*, vol. 2, edited by M. N. Hill, pp. 26-77, Wiley-Interscience, New York, 1963.

Reid, J. L., *Intermediate Waters of the Pacific Ocean*, 85 pp., *Johns Hopkins Oceanogr. Stud., 2*, Johns Hopkins Press, Baltimore, Md., 1965.

Roy, R. N., L. N. Roy, K. M. Vogel, C. Porter-Moore, T. Pearson, C. E. Good, F. J. Millero, and D. M. Campbell, The dissociation constants of carbonic acid in seawater at salinities 5 to 45 and temperatures 0 to 45°C, *Mar. Chem., 44*, 249-267, 1993.

Sabine, C. L., Geochemistry of particulate and dissolved inorganic carbon in the central North Pacific, 249 pp., Ph.D. thesis, Univ. of Hawaii, Honolulu, 1992.

Sabine, C. L., and F. T. Mackenzie, Oceanic sinks for anthropogenic CO_2, *Int. J. Energy Environ. Econ., 1*, 119-127, 1991.

Sarmiento, J. L., J. R. Toggweiler and R. Najjar, Ocean carbon cycle dynamics and atmospheric pCO_2, *Philos. Trans. R. Soc. London, 325*, 3-21, 1988.

Sarmiento, J. L., R. Murnane and C. Le Quere, Air-sea CO_2 transfer and the carbon budget of the North Atlantic, *Philos. Trans. R. Soc. London*, 348, 211-219, 1995.

Sass, E., J. W. Morse, and F. J. Millero, Dependence of values of calcite and aragonite thermodynamic solubility products on ionic models, *Am. J. Sci., 283*, 218-229, 1983.

Shiller, A. M., Calculating the oceanic CO_2 increase: A need for caution, *J. Geophys. Res., 86*, 11,083-11,088, 1981.

Stumm, W., and J. J. Morgan, *Aquatic Chemistry*, vol. 2, 780 pp., John Wiley, New York, 1981.

Sugiura, Y., Distribution of *p*H in the Kuroshio and the Oyashio regions and its oceanographical significance, *Oceanogr. Mag., 21*, 39-46, 1969.

Sverdrup, H. V., M. W. Johnson, and R. H. Fleming, *The Oceans: Their Physics, Chemistry, and General Biology*, 1087 pp., Prentice-Hall, Englewood Cliffs, N. J., 1942.

Talley, L. D., Ventilation of the subtropical North Pacific: The shallow salinity minimum, *J. Phys. Oceanogr., 15*, 633-649, 1985.

Toggweiler, J. R., and B. Samuels, Is the magnitude of the deep outflow from the Atlantic Ocean actually governed by southern hemisphere winds?, in *The Global Carbon Cycle*, edited by M. Heimann, pp. 333-366, Springer-Verlag, New York, 1993.

Toggweiler, J. R., K. Dixon and K. Bryan, Simulation of radiocarbon in a coarse-resolution world ocean model, 1, Steady state prebomb distributions, *J. Geophys. Res., 94*, 8217-8242, 1989.

Tsuchiya, M., *Upper Waters of the Intertropical Pacific Ocean*, Johns Hopkins Oceanogr. Stud. 4, 50 pp., Johns Hopkins Press, Baltimore, Md., 1968.

Tsunogai, S., and Y. Watanabe, Calcium in the North Pacific water and the effect of organic matter on the calcium-alkalinity relation, *Geochem. J., 15*, 95-107, 1981.

Tsunogai, S., H. Yamahata, S. Kudo, and O. Saito, Calcium in the Pacific Ocean, *Deep Sea Res., 20*, 717-726, 1973.

UNESCO, *Carbon Dioxide Sub-group of the Joint Panel of Oceanographic Tables and Standards*, Div. of Mar. Sci., Paris, France, 1983.

Volk, T., and M. I. Hoffert, Ocean carbon pumps: Analysis of a relative strengths and efficiencies in ocean-driven atmospheric CO_2 changes, in *The Carbon Cycle and Atmospheric CO_2: Natural Variations Archean to Present, Geophys. Monogr. Ser.*, vol. 32, edited by E. T. Sundquist and W. S. Broecker, pp. 99-110, AGU, Washington, D. C., 1985.

Wanninkhof, R., Relationship between wind speed and gas exchange over the ocean, *J. Geophys. Res., 97*, 7373-7383, 1992.

Weiss, R. F., The solubility of nitrogen, oxygen and argon in water and seawater, *Deep Sea Res., 17*, 721-735, 1970.

Winn, C. D., F. T. Mackenzie, C. L. Sabine, C. J. Carrillo, and D. M. Karl, Air-sea carbon dioxide exchange in the North Pacific: Implications for the global carbon budget, *Global Biogeochem. Cycles, 8*, 157-163, 1994.

D. M. Karl, F. T. Mackenzie, and C. Winn, School of Ocean and Earth Sciences and Technology, University of Hawaii, Honolulu, HI 96822.

C. L. Sabine, Atmospheric and Ocean Sciences Program, Department of Geological and Geophysical Sciences, Princeton University, Guyot Hall, Princeton, NJ 08544 (e-mail: sabine@weasel.princeton.edu).

(Received March 12, 1994; revised July 24, 1995;
accepted August 3, 1995.)